Small-Angle X-ray Scattering Investigation of Noncrystalline Poly(ethylene-*co*-methacrylic acid) Ionomers

Shoichi Kutsumizu,*,† Hiroyuki Tagawa,‡ Yoshio Muroga,§ and Shinichi Yano⊥

Instrumental Analysis Center, Gifu University, 1-1 Yanagido, Gifu 501-1193, Japan, Department of Applied Chemistry, Nihon University Junior College, 1-8-14 Kanda-Surugadai, Chiyoda-ku, Tokyo 101-0062, Japan, School of Engineering, Nagoya University, Furo-cho, Chikusa-ku, Nagoya 464-8603, Japan, and Department of Chemistry, Faculty of Engineering, Gifu University, 1-1 Yanagido, Gifu 501-1193, Japan

Received November 15, 1999; Revised Manuscript Received March 6, 2000

ABSTRACT: The structure of ionic aggregates in commercially important ethylene ionomers was studied by small-angle X-ray scattering (SAXS). The samples examined were sodium and zinc salts of poly(ethylene-*co*-13.3 mol % methacrylic acid) (EMAA) ionomers, which were found to be noncrystalline unlike commercially available EMAA ionomers with lower MAA contents. Not only the model fittings but also the correlation function analyses can be employed on those ionomers because of their noncrystallinity. The results clearly showed that the structure of ionic aggregate in both sodium and zinc salt ionomers can be described by Yarusso and Cooper's liquidlike model. The number of ions per aggregate was estimated on the basis of simple space-filling discussion using the data of low-molecular-mass model compounds, which reveals that the ionic core of the ionic aggregate contains anionic side groups as well as ions, and in the partially neutralized sodium salts, unneutralized COOH groups are also incorporated into the ionic aggregate. Comparisons with other EMAA ionomers with lower MAA contents than 13.3 mol % and with other ionomer systems were also discussed.

Introduction

Ionomers are ion-containing polymers containing hydrophobic backbones and a relatively small amount of ionic groups, typically acid groups neutralized with a metal cation.[1−4] It is well-known that such ionic groups tend to form phase-separated ionic aggregates in the hydrophobic polymer matrix, resulting in physical properties superior to the host polymer.[1−7] To date, many types of ionomers have been developed and examined. Among them, ethylene ionomers produced from poly(ethylene-*co*-methacrylic acid) (EMAA), which were developed by Rees et al.[1] in 1964, are still commercially very important because of their useful applications. Actually, EMAA ionomers are used as heat seal and adhesive layers in foil/paper containers and packaging films and as rubbers for golf ball covers and sports shoes, etc.[4]

The morphology of ionomers and the structure of ionic aggregates have been extensively studied by many researchers, primarily using small-angle X-ray scattering (SAXS)[8−10,12−24] and small-angle neutron scattering (SANS).[11] The SAXS profile of ionomers has two features. One is a single broad peak called the *ionic peak* usually observed at $q = 0.1-0.4$ Å^{-1} ($q = (4\pi/\lambda) \sin\theta$, where λ is the X-ray wavelength and 2θ is the scattering angle), and the other is a strong upturn in scattered intensity near $q = 0$. Several structural models have been proposed to explain these two features. The $q = 0$ upturn is assigned to the inhomogeneous distribution of ionic aggregates in ionomers.[17,19] As for the ionic peak, all the proposed models assume ionic aggregates with a dimension of 10−100 Å as the basic scattering units, but the scattering mechanisms are roughly divided into two categories: *interaggregate interference* models[8,14,15,17−23] and *intraaggregate interference* models.[9,12,13] Since the ionic peak has no fine structure and those models can produce a single broad peak, it has been very difficult to distinguish those different models. For such difficulty, Chu et al.[23b] pointed out that two similar but not the same peak profiles in *q*-space (that is, in the reciprocal space) can be significantly different when compared on the correlation function profiles in *r*-space. The most important and widely applicable model for ionic aggregates is probably Yarusso and Cooper's liquidlike model.[14] This model is based on interaggregate interference origin and successfully reproduced the ionic peak profile of *noncrystalline* sulfonated polystyrene ionomers.

The ionic peak of zinc salt EMAA ionomers was also studied by the same authors but obtained only a qualitative conclusion.[15] A reason for this is that the zinc salt EMAA ionomers examined were *semicrystalline*; in the low-*q* side, a strong peak due to the presence of polyethylene lamellae is severely overlapped with the ionic peak, which makes it difficult to extract the contribution of the ionic aggregates from the observed pattern. For the same reason, it is impossible to apply the analysis based on the correlation function profile to the EMAA ionomers. Anomalous SAXS (ASAXS) techniques are probably one solution for such inconvenience and have been employed for EMAA ionomers[20,21] as well as other ionomer systems.[19,23a] However, the detailed comparisons between the experimental data and the proposed models are inappropriate because of the low signal-to-noise ratio of the profiles.[23a]

In this paper, we report the results of SAXS studies on *noncrystalline* ethylene ionomers, which were produced from EMAA with a very high methacrylic acid

† Instrumental Analysis Center, Gifu University.
‡ Nihon University Junior College.
§ Nagoya University.
⊥ Faculty of Engineering, Gifu University.
* To whom correspondence should be addressed. E-mail kutsu@cc.gifu-u.ac.jp.

10.1021/ma991917p CCC: $19.00
Published on Web 04/22/2000

Table 1. Specific Volume (*V*) at 298 K and DSC Parameters for Various EMAA Ionomers[a]

ionomers	V/cm^3 g^{-1}	T_i/K	ΔH_i/J g^{-1}	T_m/K	ΔH_m/J g^{-1}	X_c/%
E-0.133MAA	1.0178	322	9.9	−	−	0
E-0.133MAA-0.2Na	1.0017	322	4.2	−	−	0
E-0.133MAA-0.6Na	0.9727	343	3.3	−	−	0
E-0.133MAA-1.0Na	0.9464	340	4.7	−	−	0
E-0.133MAA-0.6Zn	0.9515	334	2.5	−	−	0
E-0.075MAA-1.0Na	1.0249	325	6.3	353	3.7	1.3
E-0.054MAA-1.0Na	1.0408	324	12.8	355	15.3	5.3

[a] V, specific volume at 298 K; T_i, order−disorder transition temperature of ionic aggregates; ΔH_i, enthalpy change of the T_i peak; T_m, melting temperature of polyethylene crystallites; ΔH_m, enthalpy change of the T_m peak; X_c, degree of crystallinity of polyethylene regions; −, not found.

(MAA) content of 13.3 mol %. Since these ionomers are noncrystalline, it is possible to analyze the correlation function profile in *r*-space as well as to examine the SAXS profile in *q*-space, which could allow unambiguous determination of model parameters. This paper focuses attention on the ionic peak *q* range of these ionomers and aims at clarifying the size of the ionic aggregates and the number of ions per aggregate. The latter question has not been answered satisfactorily for EMAA ionomers, although a few reports are available only on the size.[15,20,21] Our ultimate goal is to understand the ionic aggregation in semicrystalline EMAA ionomers which are commercially very important, and we have also examined the SAXS profiles of 100% neutralized sodium salt EMAA ionomers with MAA contents of 7.5 and 5.4 mol %. These two samples have only a few percent of polyethylene crystallinity but will serve as a test for the morphological continuity between noncrystalline and semicrystalline EMAA ionomers.

Experimental Section

Materials. All the ionomer samples used in this study were kindly given to us from Du Pont-Mitsui Polychemicals Co., Ltd., Chiba, Japan. The precursor E-0.133MAA was a random copolymer of ethylene and methacrylic acid (MAA), and the MAA content was 13.3 mol %. The sodium salts and zinc salt of E-0.133MAA were prepared by a melt reaction of E-0.133MAA with a stoichiometric quantity of cation sources such as Na_2CO_3 or ZnO using a Toyoseiki Laboplastomill at 493 K for 15 min. We denote these samples in this paper as E-*m*MAA-*x*M, where *m* is the content of MAA (e.g., $m = 0.133$ means 13.3 mol % MAA) and M and *x* represent metal cation and the degree of neutralization ($0 \le x \le 1$), respectively. For comparison, 100% neutralized sodium salts of E-0.075MAA and E-0.054MAA were prepared by the same method as above and examined. Both E-0.075MAA and E-0.054MAA were semicrystalline, but the full neutralization and the quenching procedure from the melt made the sodium salts nearly noncrystalline (see below).

The samples were first vacuum-dried at 413 K for 1 h and then compression-molded into a 0.2−0.5 mm thick sheet at 423 K to be suitable for SAXS measurements. After that, the samples were rapidly cooled to room temperature in 1−2 min and stored in a vacuum desiccator at room temperature for 25−31 days prior to the measurements.

The thermal properties of E-0.133MAA ionomers were investigated by a differential scanning calorimeter (Seiko Denshi SSC-5000 system) at a heating/cooling rate of 5 K/min and summarized in Table 1. On the first heating of E-0.054MAA and E-0.075MAA ionomers aged at 293 K for about 30 days, two endothermic peaks were observed near 325 and 355 K. The higher temperature peak is clearly due to the melting of polyethylene crystallites (T_m), and the lower temperature one, which disappeared on the second heating immediately after the first cooling, is assigned to the order−disorder transition of ionic aggregates (T_i).[25] The assignment of the T_i transition is, however, not clear and still a subject of debate.[26] The enthalpy changes of the T_i and T_m peaks are denoted as ΔH_i and ΔH_m, respectively, and the degree of crystallinity in the polyethylene region (X_c) was calculated from the value of ΔH_m, by assuming that the heat of fusion of polyethylene crystallites is 290.4 J g^{-1}. The specific volume, V, at 298 K was obtained by a buoyancy method with benzene or acetonitrile. As shown in Table 1, all E-0.133MAA polymers are noncrystalline.

Measurements. SAXS experiments were carried out by using synchrotron radiation as the X-ray source at the National Laboratory for High Energy Physics, Tsukuba, Japan (Photon Factory), where the SAXS equipment for solutions (SAXES) was installed on beamline BL-10C. The storage ring was operated at an energy level of 2.5 GeV with a ring current of 250−300 mA over a period of 12 or 24 h. The SAXES employs point-focusing optics with a double-flat monochromator followed by a bent cylindrical mirror. The incident beam intensity ($\lambda = 1.488$ Å) was monitored by an ionization chamber to correct for a minor decrease in intensity during the measurements. The scattered intensity was detected by a linear position-sensitive proportional counter (PSPC) with 512 channels. The sample-to-detector distance was 620 mm, covering a scattering vector q of 0.024−0.87 Å^{-1} (0.1 Å^{-1} = 1 nm^{-1}). The geometry was further checked with chicken tendon collagen, which gives a set of sharp diffraction lines corresponding to a spacing of 653 Å. Details of the optics and instrumentation are described elsewhere.[27]

SAXS measurements were performed at room temperature, and the obtained patterns, cumulated for 500 s, were corrected for parasitic scattering (background scattering), sample absorption, and beam intensity decay and then normalized to 1 mm sample thickness. We did not measure absolute intensities, but conversion from the normalized intensities to absolute scattering units involves a simple multiplicative factor. Since the optics of the SAXES is point-focusing, the scattered intensity was not corrected for the smearing effect from finite cross section of the primary beam.

Numerical calculations including curve-fitting procedures were done on an EPSON PC-486GR personal computer with an i486SX microprocessor. The curve fittings to some structural models were carried out by using both trial-and-error method and nonlinear regression routines developed by Minami as BASIC programs,[28] where the adjustable parameters were chosen to reproduce both the scattered intensity and correlation function profiles (see below).

Results

SAXS Profiles and Correlation Functions of E-0.133MAA Ionomers. Figure 1 shows SAXS profiles of E-0.133MAA (acid form), E-0.133MAA-*x*Na ionomers with $x = 0.2$, 0.6, and 1.0, and E-0.133MAA-0.6Zn. Four salt ionomers show a broad peak called the *ionic peak* at 0.25−0.37 Å^{-1} and a strong upturn below 0.05 Å^{-1}. The former origin is the aggregation of ionic groups in the hydrophobic polyethylene matrix, and the latter is due to the inhomogeneous spatial distribution of ionic aggregates, as mentioned in the Introduction. For a given sample, the reproducibility of the peak position was within 0.02 Å^{-1} and that of the scattered intensity within 10%. The width and position of the ionic peak

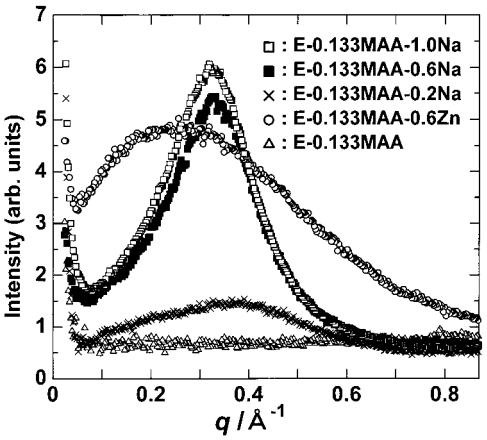

Figure 1. Plots of scattered intensity versus q for E-0.133MAA (△), E-0.133MAA-0.2Na (×), -0.6Na (■), -1.0Na (□), and -0.6Zn (○).

vary with cation and its degree of neutralization (x). As x increases, the peak position of E-0.133MAA-xNa slightly moves to lower q and becomes sharper. The peak of E-0.133MAA-0.6Zn, on the other hand, is much broader than that of E-0.133MAA-0.6Na with the same degree of neutralization. This reflects a large difference in the state of ionic aggregation between those two ionomers, which will be discussed later. In the q range of 0.05−0.08 Å^{-1}, semicrystalline EMAA ionomers such as E-0.043MAA-0.57Zn show a small peak due to the presence of polyethylene lamellae.[15,24] However, no peak was seen in that q range for E-0.133MAA polymers including the acid E-0.133MAA, which is consistent with noncrystallinity of these polymers. Since a main purpose of this study is to estimate the size of ionic aggregates and the number of ionic groups in an aggregate, we concentrate on the ionic peak q range.

It is well-known that the scattered intensity $I(q)$ is related to the electron density autocorrelation function ($\gamma(r)$) by the following equation:

$$\gamma(r) = \frac{\langle \rho(\mathbf{r}_1)\, \rho(\mathbf{r}_2) \rangle}{\langle \rho(r)^2 \rangle} = \int_0^\infty q^2 I(q) \frac{\sin(qr)}{qr}\, \mathrm{d}q \Big/ \int_0^\infty q^2 I(q)\, \mathrm{d}q \tag{1}$$

where ρ is the local electron density fluctuation and $r = |\mathbf{r}_1 - \mathbf{r}_2|$. Instead of using the $\gamma(r)$, however, an alternative function defined as

$$p(r) = r^2 \gamma(r) \tag{2}$$

is more often used, and this $p(r)$ is called the distance distribution function or simply the correlation function.[21,23b] Since SAXS can only cover a finite q range, the lower and upper limits of eq 1 (and 2) must be replaced by q_{min} and q_{max}, respectively. In the present study, $q_{min} = 0.024$ Å^{-1}, which was the lower q limit of our experiment. The peak positions in $p(r)$ did not depend on the choice of q_{min} within 0.024−0.050 Å^{-1}. $q_{max} \sim 0.8$ Å^{-1}, a point above which the contribution from ionic groups is virtually zero (depending on the samples).

To get the contribution only from ionic groups, it is necessary to subtract the contribution of amorphous polyethylene matrix (at high q) from the measured scattered intensity $I(q)$. The subtraction was done in two ways: (1) A constant background was fit to the data in the region $q = 0.84$−0.87 Å^{-1} and subtracted from the data. (2) A Vonk-like background of the form[29]

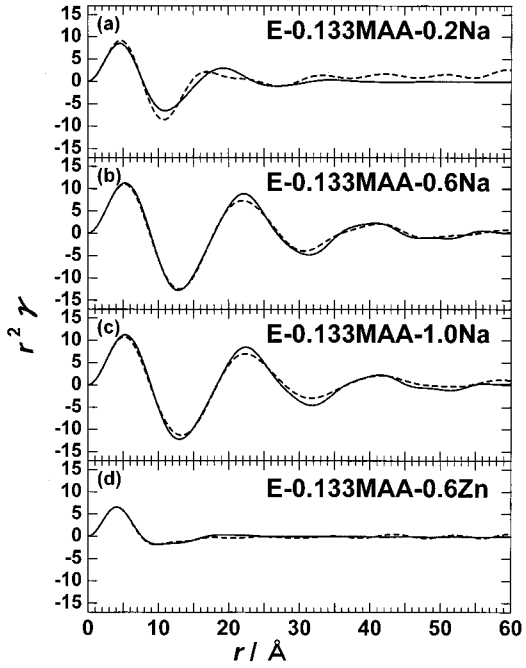

Figure 2. Plots of $r^2\gamma(r)$ versus r for (a) E-0.133MAA-0.2Na, (b) -0.6Na, (c) -1.0Na, and (d) -0.6Zn, where dotted and solid curves denote experimental and Yarusso and Cooper's liquid-like model, respectively.

$$I = A + Bq^4 \tag{3}$$

was fit to the data at q above ~0.8 Å^{-1} (around which the scattered intensity showed a weak minimum) and subtracted. For E-0.133MAA-0.6Zn, no minimum was observed in the measured range up to $q = 0.87$ Å^{-1}. Thus, to determine the q value at which a minimum is attained, q^*, the tail of the ionic peak in the range above $q = 0.6$ Å^{-1} was fit to the following polynomial function of $1/q$,

$$I = \sum a_n q^{-n} \quad (a_n \text{ is constant with } q;\ n = 0\text{−}6) \tag{4}$$

Finally, the intensity was subtracted as a constant background from the data. Although this procedure seems violent, the q^* value determined ($q^* = 1.06$ Å^{-1} with the correlation coefficient of 0.999 168) was close to the q^* value (=0.92 Å^{-1}) observed by WAXS, and therefore, the procedure is reasonable. Anyway, methods 1 and 2 mentioned above gave no appreciable difference in the behavior of $p(r)$ obtained from the subtracted data. Hereafter, the data from method 2 are used and discussed.

The $p(r)$ functions of E-0.133MAA ionomers obtained in this way are shown in Figure 2, where the broken curve of each sample was calculated from the experimental $I(q)$ using eqs 1 and 2, and the solid curve is a simulated one based on Yarusso and Cooper's liquidlike model discussed later in detail. All ionomers (broken curves) show a damping oscillation typical of a liquid structure. The behavior depends on the cation and its degree of neutralization. E-0.133MAA-0.6Na and -1.0Na show three well-defined maxima at ~5.2, ~22, and ~41 Å. E-0.133MAA-0.2Na, on the other hand, shows a well-defined peak at ~4.7 Å and a weak maximum at ~17 Å. In E-0.133MAA-0.6Zn, a maximum is seen at 4.1 Å, but above 10 Å, the $p(r)$ does not show any definite maxima, although it slightly ripples.

In the correlation functions, the first maximum from the origin is due to the interference of a single ionic aggregate itself, where the r value corresponds to the radius of the ionic core. The maxima other than the first come from the interference between aggregates, which depend on the distribution of aggregates in the matrix.[21,23b] Such information on the size and distribution is useful to select a structural model for ionic aggregates and to set the initial parameters for the fitting. As pointed out by Chu et al.,[23b] the appearance of the third maximum is very important in differentiating between *interaggregate* interference models examplified by Yarusso and Cooper's liquidlike model and *intraaggregate* interference models such as Fujimura's modified core−shell model;[13] in the modified core−shell model, no interference can be considered instead of core−core (i.e., core itself) and core−shell interferences within an aggregate. Since E-0.133MAA-xNa with x = 0.6 and 1.0 have a third maximum, it is reasonable to adapt an interaggregate interference model for the present system, and we start with Yarusso and Cooper's liquidlike model to reproduce both the correlation function and intensity profile.

According to Yarusso and Cooper's model,[14] ionic aggregates in ionomers are spherical particles that consist of an ionic core of radius R_1 and a shell of hydrocarbon chains whose radius is R_{CA}. The electron density of the ionic core is by d_1 higher than, but that of the shell is equal to, that of the polymer matrix (see Figure 8a). The spheres are dispersed in the matrix with a liquidlike order, but the closest approach between the spheres is restricted to $2R_{CA}$. The scattered intensity for their model has the form

$$I(q) = I_e N v_1^2 d_1^2 \Phi(qR_1)^2/[1 + (8v_{CA}/v_p)\Phi(2qR_{CA})] \quad (5)$$

where

$$\Phi(x) = \left[\frac{3(\sin x - x\cos x)}{x^3}\right] \quad (6)$$

and I_e is the intensity scattered by a single electron under the experimental conditions, N is the number of aggregates in the scattering volume V, $v_1 = (4\pi/3)R_1^3$, $v_{CA} = (4\pi/3)R_{CA}^3$, and $v_p = V/N$, that is, the mean sample volume occupied by each aggregate. Since we are treating a relative intensity $I_{rel}(q)$, not an absolute intensity $I(q)$, the absolute value of the preterm of Φ, and hence, of d_1, cannot be determined. Thus, confirmation of the adequacy of the model lacks some strictness, but this does not produce a serious problem for us because the shape of SAXS profiles is essentially determined by three parameters, R_1, R_{CA}, and v_p; $I_e N d_1^2$ may be replaced by a proportional factor K to adjust the intensity scale.

Figure 3 shows comparisons of simulated and experimental $I(q)$ for (a) E-0.133MAA-0.6Na and (b) E-0.133MAA-0.6Zn. The liquidlike model could fit well the measured intensity curve for both ionomers, except at $q < \sim 0.2$ Å^{-1}. For the zinc salt ionomer, the discrepancy between the simulated and measured profiles at $q < \sim 0.2$ Å^{-1} is not so small, but it was difficult to improve the fitting only by varying the parameters. Figure 4 shows the same comparisons for (a) E-0.133MAA-0.2Na and (b) -1.0Na. The ionic peaks are matched well for $q > 0.2$ Å^{-1}. The best-fit parameters obtained are summarized in Table 2, which also includes the parameters for E-0.075MAA-1.0Na and E-0.054MAA-1.0Na that will be discussed later.

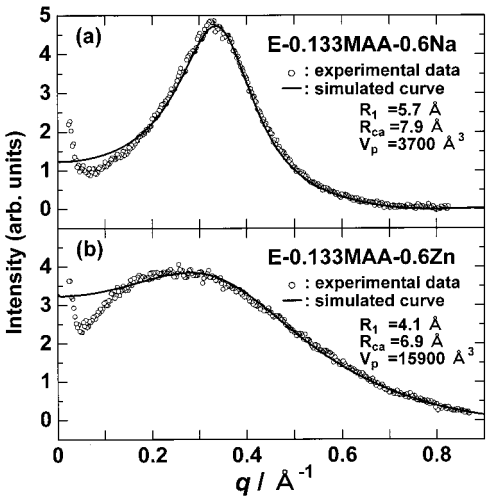

Figure 3. Comparisons of Yarusso and Cooper's liquidlike model to experimental data for (a) E-0.133MAA-0.6Na and (b) E-0.133MAA-0.6Zn, where open circles denote experimental data, and solid curves were computed on Yarusso and Cooper's liquidlike model using parameters shown in the figure.

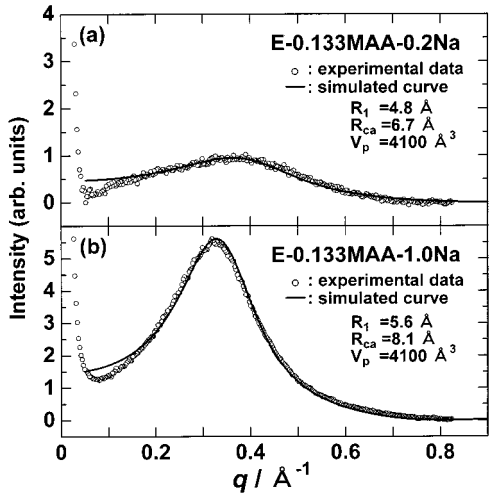

Figure 4. Comparisons of Yarusso and Cooper's liquidlike model to experimental data for (a) E-0.133MAA-0.2Na and (b) E-0.133MAA-1.0Na, where open circles denote experimental data, and solid curves were computed on Yarusso and Cooper's liquidlike model using parameters shown in the figure.

Table 2. Model Parameters for Various EMAA Ionomers[a]

ionomers	R_1/Å	R_{ca}/Å	v_p/Å^3
E-0.133MAA-0.2Na	4.8	6.7	4 100
E-0.133MAA-0.6Na	5.7	7.9	3 700
E-0.133MAA-1.0Na	5.6	8.1	4 100
E-0.133MAA-0.6Zn	4.1	6.9	15 900
E-0.075MAA-1.0Na	6.3	9.0	12 800
E-0.054MAA-1.0Na	6.2	10.5	18 000

[a] R_1, diameter of the ionic core of ionic aggregate; R_{ca}, diameter of the hydrocarbon shell of ionic aggregate; v_p, the mean volume occupied by one ionic aggregate.

As mentioned in the Introduction, to confirm the adequacy of the liquidlike model and the parameters determined, it is important to simulate the $p(r)$ function as well as the scattered intensity profile using the same model parameters. The results are shown in Figure 2. The simulated $p(r)$ (solid curve) reproduces well two maxima in E-0.133MAA-0.2Na and three maxima in E-0.133MAA-0.6Na and -1.0Na. For E-0.133MAA-0.6Zn,

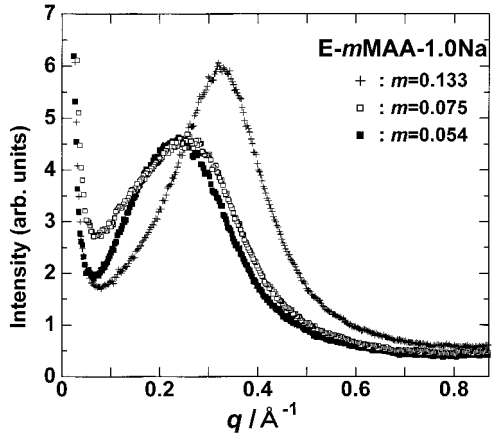

Figure 5. Plots of scattered intensity versus q for E-0.054MAA-1.0Na (■), E-0.075MAA-1.0Na (□), and E-0.133MAA-1.0Na (+).

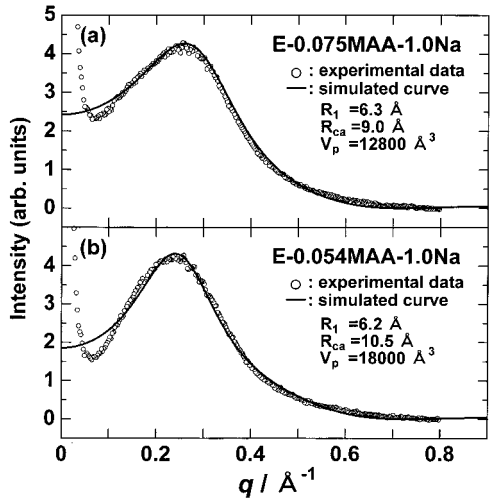

Figure 6. Comparisons of Yarusso and Cooper's liquidlike model to experimental data for (a) E-0.075MAA-1.0Na and (b) E-0.054MAA-1.0Na. Open circles denote experimental data, and solid curves were computed on Yarusso and Cooper's liquidlike model using parameters shown in the figure.

the simulated $p(r)$ gives the first maximum fairly well but at $r > \sim 20$ Å shows almost zero. As mentioned above and shown in Figure 3b, for this ionomer, the model does not fit the scattered intensity curve at $q < 0.2$ Å^{-1}, that is, at $r > 31.4$ Å. The discrepancy in q-space, however, seems not to influence so much the simulation of $p(r)$ in that r range.

SAXS Profiles and Correlation Functions of E-0.075MAA and E-0.054MAA Ionomers. Figure 5 shows SAXS patterns for fully neutralized sodium salts of EMAA containing 5.4, 7.5, and 13.3 mol % MAA. As easily seen, the ionic peaks of E-0.054MAA-1.0Na and E-0.075MAA-1.0Na are broader than that of E-0.133MAA-1.0Na. The peak position shifts from 0.24 to 0.26 and to 0.32 Å^{-1} with increasing the MAA content from 5.4 to 7.5 and to 13.3 mol %. Since the degrees of crystallinity X_c for E-0.054MAA-1.0Na and E-0.075MAA-1.0Na are a few percent (see Table 1), and the observed SAXS profiles showed no evident polyethylene lamellae peak at 0.05−0.08 Å^{-1}, the same analyses as used for E-0.133MAA ionomers are barely applicable to those two ionomers.

Figure 6 shows the fits for (a) E-0.075MAA-1.0Na and (b) E-0.054MAA-1.0Na on the basis of the liquidlike model using the parameters shown in Table 2. The

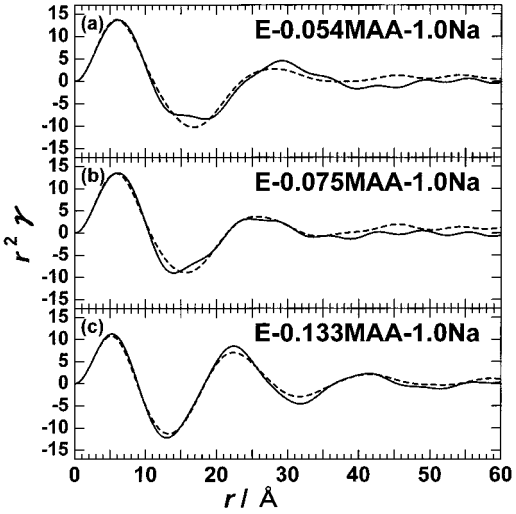

Figure 7. Plots of $r^2\gamma(r)$ versus r for (a) E-0.054MAA-1.0Na, (b) E-0.075MAA-1.0Na, and (c) E-0.133MAA-1.0Na, where dotted and solid curves denote experimental and Yarusso and Cooper's liquidlike model, respectively.

simulated curves (solid curves) almost reproduce their ionic peaks. The $p(r)$ functions for E-0.054MAA-1.0Na and E-0.075MAA-1.0Na are presented in Figure 7, where that for E-0.133MAA-1.0Na is shown again for easy comparison. The $p(r)$ of E-0.054MAA-1.0Na calculated from the experimental $I(q)$ (broken curve) shows two well-defined maxima at 6.0 and 28.1 Å, and a weak maximum at 45.5 Å, and the corresponding maxima for E-0.075MAA-1.0Na are at 5.8, 28.1, and 45.5 Å, respectively. The simulated curves (solid curves) roughly reproduce the first two maximum peaks from the origin, but not the third one, for both ionomers; the fittings of those two ionomers are not so good compared with the case of the E-0.133MAA ionomers.

Discussion

Size of Ionic Aggregates in E-MAA Ionomers. Table 2 indicates the size characteristics of ionic aggregates in EMAA ionomers: The ionic core radius R_1 is ∼5 Å, and the thickness of the hydrocarbon shell $R_{CA} - R_1$ is 40−70% of R_1. Reported values to be referred are $R_1 = 4.4$, 4.3, and 4.5 Å and $R_{CA} = 6.3$, 7.6, and 7.6 Å for E-0.043MAA-0.21Zn, E-0.043MAA-0.57Zn, and E-0.055MAA-0.59Zn,[15] respectively, and $R_1 = 3.6$ Å and $R_{CA} = 7.2$ Å for E-0.054MAA-0.17Pb(II).[21] For R_1 and R_{CA}, these values and the value obtained for E-0.133MAA-0.6Zn are in the same range. Looking closer, the ionic aggregate of sodium salt EMAA ionomers is 20−50% larger than that of the transition-metal salts, and in E-0.133MAA-xNa ionomers, the size of the ionic aggregate increases as the neutralization (x) is increased up to 0.6 but levels off with further increase. In other ionomer systems, for example, sulfonated polystyrene ionomers, the size parameters of the ionic aggregates are reported to be $R_1 = 7-11$ Å and $R_{CA} = 12-21$ Å.[14,15,19,23b] Thus, the radius R_1 of ionic aggregate of EMAA ionomers is about half of that of sulfonated polystyrene ionomers.

When varying the MAA content (m) for 100% neutralized sodium salts E-mMAA-1.0Na from 5.4 to 13.3 mol %, the size of the ionic aggregate becomes about 10% reduced. On the other hand, the value v_p of E-0.054MAA-1.0Na is 4.4 times larger than that of E-0.133MAA-1.0Na. In other words, the average density of aggregates

Table 3. Characteristic Parameters of Ionic Aggregate Estimated for Various EMAA Ionomers.

ionomers	v_1/Å^3	n_1(COO$^-$+COOH)[a]	n_2(COO$^-$)[b]	n_2(COO$^-$+COOH)[b]	β[c]	Q' [d]	$\Delta\rho$/e Å^{-3}
E-0.133MAA-0.2Na	460	5.5	1.8	9.0	0.61	499.61	0.069
E-0.133MAA-0.6Na	780	9.3	4.9	8.1	1.0	1500.61	0.093
E-0.133MAA-1.0Na	740	8.8	9.0	9.0	0.98	1763.09	0.107[e]
E-0.133MAA-0.6Zn	290	3.2	21.0	34.9	0.09	2906.7	0.395
E-0.075MAA-1.0Na	1000	11.9	16.6	16.6	0.72	1064.59	0.119
E-0.054MAA-1.0Na	980	11.7	17.4	17.4	0.67	963.34	0.131

[a] Assuming the volume per carboxylate group for sodium salt is ∼84 Å^3 and that for zinc salt is ∼91 Å^3, on the basis of the data for low-molecular-mass model compounds. [b] Assuming all ions in a volume of v_p are incorporated into an ionic aggregate. [c] Fraction of side groups (including both carboxylate and carboxylic acid groups) that are in aggregates. [d] In arbitrary intensity unit times Å^{-3}, calculated by using eq 10. [e] Calculated from n_1(COO$^-$+COOH) and v_1 of E-0.133MAA-1.0Na. $\Delta\rho$ for other samples were directly calculated from the values of v_1, v_p, and Q' by using $k = 1.8959 \times 10^{-5}$ and eqs 9 and 10 (see text).

is greatly increased with increasing the MAA content. A similar tendency was reported for sulfonated polystyrene ionomers.[14,15]

Number of Ions per Aggregate in E-MAA Ionomers. How many ions are contained on average in an aggregate? This simple but important question has not been answered satisfactorily so far especially for commercially important EMAA ionomers. A reason for this is that determination of the size of ionic aggregate does not necessarily lead to the estimation of the number of ions per aggregate; to estimate the number of ions per aggregate, it is necessary to solve a question of whether either only ions or both ions and carboxylate groups (i.e., as ion pairs) are contained in an ionic core of a radius of R_1. To solve this question, the following two methods were used to estimate the number of ions per aggregate and compared with each other.

In the first method, it was assumed that each ion pair occupies the same volume as in crystals of low-molecular-mass sodium or zinc acetate. The validity for using low-molecular-mass acetates as the model compounds is supported by previous extended X-ray absorption fine structure (EXAFS) studies,[30] which clearly show that the local order around the cation is very close to that in the low-molecular-mass compounds. Several crystallographic data, those for NaH(CH$_3$COO)$_2$,[31] Zn(CH$_3$COO)$_2$·2H$_2$O,[32] Zn(CH$_3$COO)$_2$,[33,34] and Zn$_4$O(CH$_3$COO)$_6$,[35] are available, and the volume per Na(CH$_3$COO) (denoted as v[Na(CH$_3$COO)]) and the volume per Zn$_{1/2}$(CH$_3$COO) (v[Zn$_{1/2}$(CH$_3$COO)]) can be estimated on the basis of the unit cell volume and the number of formula unit per unit cell volume. The result was v[Na(CH$_3$COO)] ∼ 84 Å^3 and v[Zn$_{1/2}$(CH$_3$COO)] ∼ 91 Å^3 (on average). For an ionic aggregate with a core volume of v_1, the number of ion pairs contained in the aggregate is obtained by using a relation of v_1/v[Na(CH$_3$COO)] or v_1/v[Zn$_{1/2}$(CH$_3$COO)]. The value obtained in this way is denoted as n_1(COO$^-$ + COOH), where "COO$^-$ + COOH" means that the number also includes the number of unneutralized carboxylic acid COOH groups in an aggregate and the suffix 1 represents the number of this estimation method. At first sight, the n_1(COO$^-$ + COOH) value might be smaller than the real value, because v[Na(CH$_3$COO)] or v[Zn$_{1/2}$(CH$_3$COO)] includes not only the volume of carboxylate salt groups but also the volume of methyl group. Such overestimation for v[Na(CH$_3$COO)] or v[Zn$_{1/2}$(CH$_3$COO)] seems to be canceled out by a relatively low ordered organization inside ionic aggregates, because n_1(COO$^-$ + COOH) was found to be a fairly reasonable value, as will be shown below.

v_p is the sample volume per aggregate, and the second method involves an assumption that all ionic groups in the volume of v_p are incorporated into an ionic aggregate. In this case, the v_p may be related to n_2(COO$^-$ + COOH) by the following equation:

$$n_2(\mathrm{COO}^- + \mathrm{COOH}) = mN_A\rho v_p/\mathrm{EW} \qquad (7)$$

Here, m is the fraction of the MAA content, N_A is Avogadro's number, ρ is the polymer density (g/Å^3), calculated by using the specific volume data in Table 1, and EW is the ionomer equivalent weight (g/mol). For E-0.133MAA-1.0Na, for example, EW = 38.70 because the formula unit of E-0.133MAA-1.0Na is given by (CH$_2$-CH$_2$)$_{0.867}$(CH$_2$C(CH$_3$)COONa)$_{0.133}$. The n_2(COO$^-$) was calculated by multiplying n_2(COO$^-$ + COOH) by the degree of neutralization, x. In the second method, both n_2(COO$^-$ + COOH) and n_2(COO$^-$) should be regarded as the upper limits of each value.

Table 3 lists n_1(COO$^-$ + COOH), n_2(COO$^-$ + COOH), and n_2(COO$^-$). The following four points should be noted: (1) In each of ionomer samples, the n_1(COO$^-$ + COOH) never exceeds the n_2(COO$^-$ + COOH) within experimental error; the values of n_1(COO$^-$ + COOH) satisfy a necessary condition that n_2(COO$^-$ + COOH) is the upper limit. Assuming that the real volume of v[Na(CH$_3$COO)] is smaller than 84 Å^3, the obtained n_1(COO$^-$ + COOH) for E-0.133MAA-0.6Na and -1.0Na would be beyond the n_2(COO$^-$ + COOH). Thus, it is concluded that the overestimation for v[Na(CH$_3$COO)] or v[Zn$_{1/2}$(CH$_3$COO)] is negligible, although the estimation method 1 is fairly rough.

(2) The volume of sodium cation with an ionic radius of 1.33 Å is ∼10 Å^3. Thus, if the ionic core of a radius of R_1 contained only metal cations, the number of sodium cations per aggregate would be much (about 8 times!) larger than the corresponding n_1(COO$^-$ + COOH). This is unrealistic because the sample never contains such a large number of ions. Therefore, one can reach an important conclusion that the ionic core contains anionic side groups as well as metal cations. Of course, it is easy to understand that a particle containing both metal cations and anionic side groups is more energetically favorable than the one only containing ions.

(3) In E-0.133MAA-0.2Na, the number of carboxylate groups in volume v_p, that is, the n_2(COO$^-$), is only 1.8, which is much smaller than the n_1(COO$^-$ + COOH). The same situation is also seen for E-0.133MAA-0.6Na. These observations indicate an interesting fact that not only carboxylate ion pairs (e.g., −COO$^-$Na$^+$) but also unneutralized carboxylic acid groups −COOH are incorporated into ionic aggregates, and this is the reason the number estimated by method 1 is denoted as n_1(COO$^-$ + COOH). The idea that in *partially* neutralized sodium salts of EMAA ionomers the ionic aggregate contains unneutralized −COOH was first proposed by Hirasawa et al., who considered that the optimal number of oxygen atoms around Na$^+$ is 6, as realized

in $NaH(CH_3COO)_2$,[31] which needs a hexacoordination structure like $(COO^-)Na(COOH)_2$;[36] at x larger than 0.33, some of oxygen atoms would be shared by neighboring two Na^+ cations to satisfy the coordination number of 6. Vanhoorne and Register pointed out that in melt rheology the presence of unneutralized acid groups is important for substantially reducing the melt viscosity of the sodium ionomers.[37]

(4) In E-0.133MAA-0.6Na and -1.0Na, all ion pairs (including unneutralized carboxylic acid groups in the former case) are incorporated into ionic aggregates, because the $n_1(COO^- + COOH)$ is almost equal to (or even a little bit larger than) the $n_2(COO^- + COOH)$. The parameter β is used to describe the fraction of side groups that are in aggregates, and for E-0.133MAA-0.6Na and -1.0Na, $\beta \sim 1.0$. The β for E-0.133MAA-0.2Na is ~0.6, and the β for E-0.075MAA-1.0Na and E-0.054MAA-1.0Na are also almost the same. For E-0.133MAA-0.6Zn, very surprisingly, the $n_1(COO^- + COOH)$ is only 3.2, and this means that an ionic aggregate contains at most two zinc ions. Only 10% of ions are present in ionic aggregates in this zinc salt ionomer.

Electron Density of Ionic Core of Aggregates in the Sodium Salt and Zinc Salt EMAA Ionomers. Noncrystalline EMAA ionomers are considered as a two-phase system, which consists of ionic aggregate and polymer amorphous phases. Provided that the ionic aggregate phase with the volume fraction ϕ_i has sharp boundaries with the amorphous phase, the electron density difference $\Delta\rho$ between those two phases can be obtained from the following SAXS invariant Q:[38,39]

$$Q = \int_0^\infty q^2(I(q)/I_e V)\,dq = 2\pi^2(\Delta\rho)^2\phi_i(1-\phi_i) \quad (8)$$

Here, the upper and lower limits of the integral are replaced by q_{max} and q_{min} as in eq 1, when the calculation is made. Using the model parameters v_1 and v_p, eq 8 may be rewritten as

$$Q = \int_0^\infty q^2(I(q)/I_e V)\,dq = 2\pi^2(\Delta\rho)^2(v_1/v_p)(1-(v_1/v_p)) \quad (9)$$

Since we measured only the relative intensities $I_{rel}(q)$, not the absolute intensities $I(q)$ in eq 8 or 9, it is necessary to determine the proportional factor k by eq 10, under a constant volume of V:

$$Q = kQ' = k\int_0^\infty q^2\, I_{rel}(q)\,dq \quad (10)$$

The value of k was determined by using the data for E-0.133MAA-1.0Na: First, Q' in eq 10 was calculated and found to be 1763.09 in arbitrary intensity units times $Å^{-3}$. For E-0.133MAA-1.0Na, nine COONa groups are present in an aggregate with a volume of 740 $Å^3$, thereby producing the electron density ρ_i:

$$\rho_i = (33e \times 9)/(740\ Å^3) = 0.401\ e/Å^3$$

Amorphous poly(ethylene), on the other hand, should have an electron density of $\rho_a = 0.294\ e/Å^3$, on the basis of mass density of 0.855 g cm^{-3}.[40] Assuming that the amorphous phase of E-0.133MAA-1.0Na consists of pure polyethylene, the electron density difference was calculated as $\Delta\rho = \rho_i - \rho_a = 0.107\ e/Å^3$, and then Q was obtained using v_1 and v_p of E-0.133MAA-1.0Na. Finally, from eq 10, $k = 1.8959 \times 10^{-5}$ was obtained. For other ionomer samples, the electron density differences $\Delta\rho$ were estimated on the basis of this k, which are listed in Table 3.

The above circuitous estimation of $\Delta\rho$ values is based on many assumptions and probably contains considerable errors. To check that estimated $\Delta\rho$ values are adequate, the electron densities of low-molecular-mass model compounds were also calculated. For the sodium salt ionomers, the model compound is $NaH(CH_3COO)_2$,[31] whose electron density is 0.440 e/$Å^3$. Provided that the ionic aggregate in the sodium salts has a structure similar to this crystal analogue, the electron density difference should be 0.146 e/$Å^3$. The $\Delta\rho$ values for the sodium salt ionomers are 50−90% of this value, and at this point, the $\Delta\rho$ are physically reasonable, which also confirms that the model parameters obtained from this SAXS study are physically adequate.

The average electron density of four low-molecular-mass zinc acetates ($Zn(CH_3COO)_2{\cdot}2H_2O$,[32] orthorhombic $Zn(CH_3COO)_2$,[33] monoclinic $Zn(CH_3COO)_2$,[34] and $Zn_4O(CH_3COO)_6$[35]) is 0.550 ± 15 e/$Å^3$, and therefore for the zinc salt ionomer, the upper limit of the electron density difference of the ionic aggregate is 0.256 e/$Å^3$. The obtained $\Delta\rho$ value for E-0.133MAA-0.6Zn was, however, 0.395 e/$Å^3$. Since the electron density of the low-molecular-mass model compounds is a value averaged throughout the unit cell, it is in principle possible that the local electron density inside the ionic aggregate is beyond this value (and in this case, zinc carboxylates are more closely packed in the ionic aggregate than in low-molecular-mass crystals). Even considering this possibility, the $\Delta\rho$ of E-0.133MAA-0.6Zn seems too high and unrealistic. The reason for this is, first, that the assumption of clear phase boundaries between the ionic aggregate and amorphous phases is not valid for this ionomer; less clear phase boundaries would lower the value of k to make $\Delta\rho$ close to a reasonable value. Actually, the present study showed $\beta = 0.09$, suggesting that a considerable amount of ions is dispersed in the polymer matrix, which would make phase boundaries diffuse. A second possibility is that uncertainty of background correction for E-0.133MAA-0.6Zn probably may produce some undesirable situation on estimating Q', resulting in a considerable error in the $\Delta\rho$. Both situations may be realized, but the first one is probably a major factor.

Spatial Arrangement of Ionic Aggregates in EMAA Ionomers and Related Measurements. The spatial arrangement of ionic aggregates in E-0.133MAA-0.6Zn is quite different from that in E-0.133MAA-0.6Na. The $p(r)$ function of the sodium salt ionomer shows three well-defined maxima, whereas for the zinc salt ionomer, only the first maximum is clearly visible. Moreover, the v_p value for the zinc salt ionomer is 4.3 times as large as that for the sodium salt ionomer. Therefore, the following picture may be visualized: in the sodium salt ionomer, the ionic aggregate has a relatively large chance of being neighbored with other aggregates, whereas in the zinc salt ionomer, the ionic aggregates are almost isolated and dispersed in the amorphous phase. Such a picture of the spatial arrangement is supported by our dielectric results.[41] The sodium salt ionomer exhibits two glass transitions (T_g): one is at 284 K, measured at 1 kHz, for the polyethylene matrix phase, and the other is at 383 K for the ionic aggregate phase (*ionic cluster*, in Eisenberg's terminology[7]), whereas the zinc salt ionomer shows only one T_g at 347 K at 1

kHz, which is assigned to ionic aggregates dispersed in the amorphous phase. In other words, in the zinc salt ionomer, the formation of ionic aggregates is not so large as to have its own T_g on the dielectric relaxations.

Comparison with Noncrystalline Sulfonated Polystyrene Ionomers. For sulfonated polystyrene ionomers,[23b] it was observed that the 100% neutralized sodium and zinc salts exhibit a typical ionic peak at 0.16 and 0.18 Å^{-1}, respectively. Their correlation function profiles showed four maxima, thus indicating that the spatial arrangements of ionic aggregates are very similar for these two ionomers. The model fitting in both *q*- and *r*-spaces provided the following structural parameters for the liquidlike model: $R_1 = 8.5$ Å, $R_{CA} = 16$ Å, and $v_p = 40\,000$ Å^3 for the sodium salt and $R_1 = 7.5$ Å, $R_{CA} = 15$ Å, and $v_p = 60\,000$ Å^3 for the zinc salt. In sulfonated polystyrene ionomers, the size of ionic aggregate in the zinc salt is slightly smaller than that in the sodium salt, but the difference between the two salts is not so significant, in contrast with that in EMAA ionomers. Such different behavior of ionic aggregation between those two ionomer systems is primarily due to the fact that sulfonic acid is much stronger than carboxylic acid. In EMAA ionomers with the weakly acidic side group, the difference in the bonding nature between the COO^- side group and metal cation, that is, ionic in the sodium salts while rather covalent in the zinc salt, seems to be pronounced and important in the ionic aggregations, which is a characteristic of EMAA ionomers.

Ionic Aggregates of the Zinc Salt Ionomers. As for the ionic aggregate in the zinc salt EMAA ionomers, we should refer to the recent report by Laurer and Winey.[42] For two ionomers with a MAA content of 5.4 mol % (E-0.054MAA-0.22Zn and -0.58Zn), the size of the zinc-rich domains was estimated at 25−28 Å from the scanning transmission electron microscopic (STEM) observations in high-angle annular dark field (HAADF) and bright field (BF) modes. Moreover, it was pointed out that the domains are nearly spherical and have a narrow size distribution. In the $p(r)$ function of E-0.133MAA-0.6Zn (in Figure 2d), however, no evidence for "clustering" of ionic aggregates was found around 25 Å, around which a very weak second maximum is only barely visible (at about 17 Å). Such unclearness of the second maximum is partly due to a very low density of ionic aggregates in the polymer matrix, as already pointed out, and partly due to a broad size distribution of the ionic aggregates. Although their samples and E-0.133MAA-0.6Zn examined in this study are different in the MAA content, which makes the former samples semicrystalline whereas the latter noncrystalline, the discrepancy between their conclusions and our results on the size and distribution of ionic aggregates is certainly to be reconsidered. Moreover, for E-0.133MAA-0.6Zn, the liquidlike model did not fit well the scattering profile at $q < 0.2$ Å^{-1}.

For these problems, we tried to modify the liquidlike model. Possible alterations are (1) aggregate shape, (2) electron density profile, (3) spatial distribution, and (4) size distribution. Concerning the shape, there is no plausible reason for taking other shapes than sphere. As for the spatial distribution, Lee et al. proposed the bead−spring micronetwork model for polyurethane ionomers with the ionic groups regularly spaced. By taking a strong correlation between the neighboring aggregates into consideration, the high-q shoulder region of the ionic peak was successfully accounted for.[18] This is, however, not the case for E-0.133MAA-0.6Zn, because it is a random copolymer ionomer, and the ionic peak does not exhibit such a shoulder at high q. Among the remaining two factors, the electron density profile, the third alteration, was reexamined in this study.

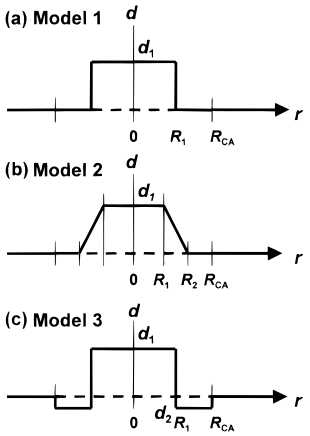

Figure 8. Density profiles of three liquidlike models: (a) model 1, original Yarusso and Cooper's model; (b) model 2, where the electron density decreases linearly from R_1 to R_2; (c) model 3, where the electron density of the hydrocarbon shell is by $-d_2$ ($d_2 < 0$) lower than that of the polymer matrix.

Figure 8 illustrates three cases of the electron density profiles within and around an ionic aggregate in ionomers. Model 1 in (a) is the original model by Yarusso and Cooper.[14] When moving away from the ionic core to the amorphous region, the electron density might decrease gradually in the vicinity of the boundary, and model 2 in (b) assumes that this decrease is linear along with the direction r from R_1 to R_2; R_2 is an additional parameter. The scattered intensity $I(q)$ has the form

$$I(q) = I_e N d_1^2 [R_1 v_1 \Psi(qR_1) - R_2 v_2 \Psi(qR_2)]^2 / (R_2 - R_1)^2 [1 + (8v_{CA}/v_p)\Phi(2qR_{CA})] \quad (11)$$

where

$$\Psi(x) = \frac{3(x \sin x + 2 \cos x)}{x^4} \quad (12)$$

and other valuables have the same meaning as in eq 5. In model 3 in (c), in turn, it is postulated that the electron density of the shell consisting of polyethylene backbones attached to an ionic aggregate is by $-d_2$ ($d_2 < 0$) lower than the density of the polymer matrix. This situation may be especially realized in ionomers whose amorphous phase contains a considerable amount of isolated ionic groups, as in E-0.133MAA-0.6Zn. The scattered intensity $I(q)$ has the form

$$I(q) = I_e N [v_1(d_1 - d_2)\Phi(qR_1) + v_2 d_2 \Phi(qR_2)]^2 / [1 + (8v_{CA}/v_p)\Phi(2qR_{CA})] \quad (13)$$

Figure 9 compares these three models (a) in q-space and (b) in r-space. The model fit parameters are listed in Table 4. Unfortunately, no significant difference was observed among those three models, and none of the three is said to be better; better matching at $q < 0.2$ Å^{-1} cannot be accomplished by changing the electron density profile, and all the models show that the size of ionic aggregate in E-0.133MAA-0.6Zn is on the order of

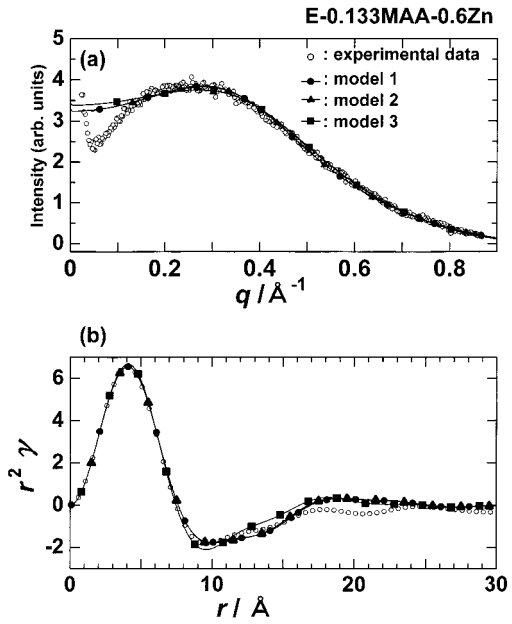

Figure 9. Comparison of three liquidlike models postulated for E-0.133MAA-0.6Zn: (a) plots of the scattered intensity versus q and (b) plots of $r^2\gamma(r)$ versus r. Models 1−3 are described in the text, and the parameters for each computed curve are listed in Table 4. In (a), note that the computed curves for models 1 and 2 are completely overlapped with each other.

Table 4. Comparison of Model Parameters of Three Liquidlike Models for E-0.133MAA-0.6Zn[a]

models	R_1/Å	R_2/Å	d_2/d_1	R_{ca}/Å	v_p/Å^3
1	4.1			6.9	15 900
2	3.5	4.6		6.8	15 000
3	4.3		−0.0394	6.2	13 230

[a] The details of the three models and the meanings of the model parameters R_1, R_2, d_1, d_2, R_{ca}, and v_p are described in the text and in Figure 8.

10 Å. A new model is desired, and probably, it is necessary to take the polydispersity of ionic aggregate size, the fourth alteration, into consideration. However, in the framework of interaggregate interference models, that would be very difficult. Further studies are currently under way in our laboratories.

Conclusions

The structure of ionic aggregates in the sodium and zinc salt ionomers of poly(ethylene-*co*-13.3 mol % methacrylic acid) (E-0.133MAA) and two sodium salts of EMAA (E-0.075MAA-1.0Na and E-0.054MAA-1.0Na) have been investigated by SAXS. Unlike commercially available EMAA ionomers, the E-0.133MAA polymers were noncrystalline because of the very high MAA content of 13.3 mol %, and the latter two salts were barely noncrystalline. For such noncrystalline ethylene ionomers, both correlation function [$p(r)$] analysis and model fitting can be employed. The results showed that the structure of ionic aggregate in both sodium and zinc salt ionomers could be described by Yarusso and Cooper's liquidlike model.

An important conclusion obtained in this study is that the ionic core of the ionic aggregate contains anionic side groups as well as ions. The number of anionic side groups per aggregate has been estimated at 6−12 for the sodium salts of EMAA ionomers and at only 3 for the zinc salt. In partially neutralized sodium salts of E-0.133MAA, it has been revealed that unneutralized COOH groups are also incorporated into the ionic aggregates. The $p(r)$ function of E-0.133MAA-0.6Na ionomer showed three well-defined maxima, whereas for the E-0.133MAA-0.6Zn ionomer, only the first maximum was clearly visible. This result gives us a picture that in the sodium salt ionomer the ionic aggregate has a larger chance of being neighbored with other aggregates, whereas in the zinc salt ionomer, the ionic aggregates, which contain only 3−4 carboxylate groups, are almost isolated and dispersed in the matrix. In EMAA ionomers, the difference in the bonding nature of COO− metal cation, that is, ionic in the sodium salts while rather covalent in the zinc salt, seems to be pronounced and important in the ionic aggregation. This is in contrast with the case of sulfonated polystyrene ionomers, where the ionizable side groups are sulfonic acid, much stronger than carboxylic acid, and thus able to form a larger ionic aggregate with about a double size and with no significant difference in the ionic aggregation behavior for different cations. From the examination of E-0.075MAA-1.0Na and E-0.054MAA-1.0Na, morphological continuity was seen from noncrystalline E-0.133MAA to essentially semicrystalline E-0.075MAA and E-0.054MAA ionomers, and therefore, our new insights obtained in this study would be valid for the structure of ionic aggregates in commercially available EMAA ionomers with lower MAA contents.

A problem of mismatch between the simulated and measured SAXS profiles at $q < \sim 0.2$ Å^{-1}, especially seen for the zinc salt ionomer, remains, which is the next subject to be solved.

Acknowledgment. We thank Dr. Eisaku Hirasawa (now at Fujimori-Kogyo Co.), Mr. Yoshikazu Kutsuwa, Dr. Hitoshi Tachino, and Mr. Hisaaki Hara of Du Pont-Mitsui Polychemicals Co., Chiba, Japan, for kindly giving us ionomer samples and their very helpful discussions and encouragement and Prof. Kenji Tadano of Gifu College of Medical Technology for the measurements of specific volumes and his valuable suggestions and discussions. We also thank Mr. Tomomi Ikeno and Mr. Shunichi Osada of Gifu University for their helps in SAXS measurements and Mr. Masahiro Goto of Gifu University for his experimental aid. This work was partly supported by Grant-in-Aid for Scientific Research (No. 07650797) from the Ministry of Education, Science, and Culture, Japan, and has been performed under the approval of the Photon Factory Program Advisory Committee (proposal 94G125). Prof. Katsumi Kobayashi of the National Laboratory for High Energy Physics is greatly thanked for his guidance and kind help.

References and Notes

(1) (a) Rees, R. W.; Vaughan, D. J. *Polym. Prepr.* (*Am. Chem. Soc., Div. Polym. Chem.*) **1965**, *6*, 287. (b) Rees, R. W.; Vaughan, D. J. *Polym. Prepr.* (*Am. Chem. Soc., Div. Polym. Chem.*) **1965**, *6*, 296.

(2) *Ionic Polymers*; Holliday, L., Ed.; Applied Science: London, 1975.

(3) (a)Eisenberg, A.; King, M. *Ion-Containing Polymers, Physical Properties and Structure, Polymer Physics*; Academic Press: New York, 1977; Vol. 2. (b) *Structure and Properties of Ionomers*; Pineri, M., Eisenberg, A., Eds.; NATO ASI Series C, Mathematical and Physical Sciences; D. Reidel: Dordrecht, The Netherlands, 1987; Vol. 198.

(4) *Ionomers: Characterization, Theory, and Applications*; Schlick, S., Ed.; CRC Press: Boca Raton, FL, 1996.

(5) Longworth, R.; Vaughan, D. J. *Nature (London)* **1968**, *218*, 85.

(6) Eisenberg, A. *Macromolecules* **1970**, *3*, 147.
(7) Eisenberg, A.; Hird, B.; Moore, R. B. *Macromolecules* **1990**, *23*, 4098.
(8) Marx, C. L.; Caulfield, D. F.; Cooper, S. L. *Macromolecules* **1973**, *6*, 344.
(9) (a) MacKnight, W. J.; Taggart, W. P.; Stein, R. S. *J. Polym. Sci., Polym. Symp.* **1974**, *45*, 113. (b) Kao, J.; Stein, R. S.; MacKnight, W. J.; Taggart, W. P.; Cargill, G. S. III *Macromolecules* **1974**, *7*, 95.
(10) Moudden, A.; Levelut, A.-M.; Pineri, M. *J. Polym. Sci., Polym. Phys. Ed.* **1974**, *15*, 1707.
(11) Meyer, C. T.; Pineri, M. *J. Polym. Sci., Polym. Phys. Ed.* **1978**, *16*, 569.
(12) Roche, E. J.; Stein, R. S.; Russell, T. P.; MacKnight, W. J. *J. Polym. Sci., Polym. Phys. Ed.* **1980**, *18*, 1497.
(13) Fujimura, M.; Hashimoto, T.; Kawai, H. *Macromolecules* **1981**, *14*, 1309.
(14) Yarusso, D. J.; Cooper, S. L. *Macromolecules* **1983**, *16*, 1871.
(15) Yarusso, D. J.; Cooper, S. L. *Polymer* **1985**, *26*, 371.
(16) Weiss, R. A.; Lefelar, J. A. *Polymer* **1986**, *27*, 3.
(17) Williams, C. E.; Russell, T. P.; Jérôme, R.; Horrison, J. *Macromolecules* **1986**, *19*, 2877.
(18) Lee, D.-C.; Register, R. A.; Yang, C.-Z.; Cooper, S. L. *Macromolecules* **1988**, *21*, 998.
(19) Ding, Y. S.; Hubbard, S. R.; Hodgson, K. O.; Register, R. A.; Cooper, S. L. *Macromolecules* **1988**, *21*, 1698.
(20) Register, R. A.; Cooper, S. L. *Macromolecules* **1990**, *23*, 318.
(21) Chu, B.; Wu, D. Q.; Mahler, W. *Mater. Res. Soc. Symp. Proc.* **1990**, *171*, 237.
(22) Moore, R. B.; Bittencourt, D.; Gauthier, M.; Williams, C. E.; Eisenberg, A. *Macromolecules* **1991**, *24*, 1376.
(23) (a) Chu, B.; Wu, D. Q.; Lundberg, R. D.; MacKnight, W. J. *Macromolecules* **1993**, *26*, 994. (b) Wu, D. Q.; Chu, B.; Lundberg, R. D.; MacKnight, W. J. *Macromolecules* **1993**, *26*, 1000.
(24) Quiram, D. J.; Register, R. A.; Ryan, A. J. *Macromolecules* **1998**, *31*, 1432.
(25) (a) Tadano, K.; Hirasawa, E.; Yamamoto, Y.; Yamamoto, H.; Yano, S. *Jpn. J. Appl. Phys.* **1987**, *26*, L1440. (b) Tadano, K.; Hirasawa, E.; Yamamoto, H.; Yano, S. *Macromolecules* **1989**, *22*, 226. (c) Hirasawa, E.; Yamamoto, Y.; Tadano, K.; Yano, S. *Macromolecules* **1989**, *22*, 2776.
(26) Goddard, R. J.; Grady, B. P.; Cooper, S. L. *Macromolecules* **1994**, *27*, 1710.
(27) Ueki, T.; Hiragi, Y.; Kataoka, M.; Inoko, Y.; Amemiya, Y.; Izumi, Y.; Tagawa, H.; Muroga, Y. *Biophys. Chem.* **1985**, *23*, 115.
(28) Minami, S. *Processing of Wave Signals for Scientific Measurements*; CQ Press: Tokyo, 1986 [in Japanese].
(29) Kortleve, G.; Tuynman, C. A.; Vonk, C. G. *J. Polym. Sci., Part A2* **1972**, *10*, 123.
(30) For example: (a) Yarusso, D. J.; Ding, Y. S.; Pan, H. K.; Cooper, S. L. *J. Polym. Sci., Polym. Phys. Ed.* **1984**, *22*, 2073. (b) Vlaic, G.; Williams, C. E.; Jérôme, R.; Tant, M. R.; Wilkes, G. L. *Polymer* **1988**, *29*, 173.
(31) Speakman, J. C.; Mills, H. H. *J. Chem. Soc.* **1961**, 1164.
(32) van Niekerk, J. N.; Schoening, F. R. L.; Talbot, J. H. *Acta Crystallogr.* **1953**, *6*, 720.
(33) Capilla, A. V.; Aranda, R. A. *Cryst. Struct. Commun.* **1979**, *8*, 795.
(34) Clegg, W.; Little, I. R.; Straughan, B. P. *Acta Crystallogr.* **1986**, *C42*, 1701.
(35) Koyama, H.; Saito, Y. *Bull. Chem. Soc. Jpn.* **1954**, *27*, 112.
(36) Hirasawa, E.; Yamamoto, Y.; Tadano, K.; Yano, S. *J. Appl. Polym. Sci.* **1991**, *42*, 351.
(37) Vanhoorne, P.; Register, R. A. *Macromolecules* **1996**, *29*, 598.
(38) *Small Angle X-ray Scattering;* Glatter, O., Kratky, O., Eds.; Academic Press: London, 1982.
(39) Feigin, L. A.; Svergun, D. I. *Structure Analysis by Small-Angle X-ray and Neutron Scattering;* Plenum Press: New York, 1987.
(40) *Polymer Handbook*, 2nd ed.; Brandrup, J., Immergut, E. H., Eds.; John Wiley and Sons: New York, 1975.
(41) (a) Tadano, K.; Kutsumizu, S.; Yano, S.; Hara, H.; Tachino, H.; Kutsuwa, Y.; Hirasawa, E. *Polym. Prepr. Jpn.* **1994**, *43*, 3501 [in Japanese]. (b) Kutsumizu, S.; Tadano, K.; Matsuda, Y.; Goto, M.; Tachino, H.; Hara, H.; Hirasawa, E.; Tagawa, H.; Muroga, Y.; Yano, S., submitted to *Macromolecules*.
(42) Laurer, J. H.; Winey, K. I. *Macromolecules* **1998**, *31*, 9106.

MA991917P